Chapter 6

Wing Design

This chapter deals with some of the considerations involved in wing design, especially the selection of basic sizing parameters. There are a number of important trade-offs associated with these parameters, each one of which affects drag, structural weight, stalling characteristics, fuel volume, off-design performance, and other characteristics.

There are two approaches to wing design:

1. Find planform and twist distribution that minimize a combination of drag and weight, while satisfying $C_{L_{\max}}$ constraints.
2. Select a desirable lift distribution and then compute the twist, taper, and thickness distributions to achieve it.

The latter approach is only viable when the designer has enough experience to know what constitutes a desirable lift distribution. The first approach is often combined with numerical optimization.

Wing lift distribution is an important consideration in wing design. The spanwise lift distribution is closely related to the wing geometry and determines wing performance characteristics such as induced drag, structural weight, and stalling characteristics. A reasonable lift and C_l distribution provides a good starting point in the design of a wing.

6.1 Wing Design Parameters

The major wing design parameters can be divided into two levels. The first level design parameters are generally more influential and should be determined first. They are:

- Span
- Area
- Thickness
- Sweep

The second level design parameters are important, but they can be determined at a later stage because the trade-offs between the first level design parameters and the rest of the aircraft are more crucial, and can be made assuming that a set of second level parameters can be determined such that the wing performs as expected. The second level parameters are:

- Taper

- Airfoil shape(s)
- Twist
- Tip shape

In this section, we will discuss the effect that each of these variables has on drag, structural weight, etc., before describing a procedure for performing the actual design. Some of these parameters are illustrated in Fig. 6.1.

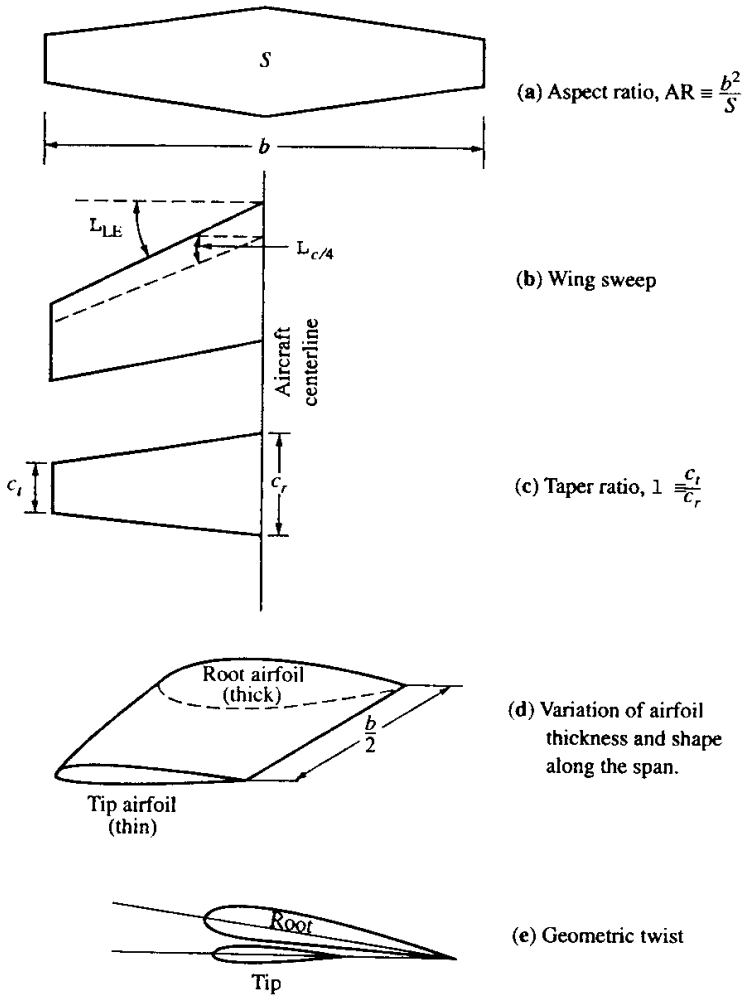

Figure 6.1: Wing planform design parameters (Anderson Jr., 1999, Fig. 8.6)

6.1.1 Span

Selecting the wing span is one of the most basic decisions to made in the design of a wing. The span is sometimes constrained by contest rules, hangar size, or ground facilities but when it is not we might decide to use the largest span consistent with structural dynamic constraints (flutter). This would reduce the induced drag directly.

However, as the span is increased, the wing structural weight also increases and at some point the weight increase offsets the induced drag savings. This point is rarely reached, though, for several reasons:

1. The optimum is quite flat and one must stretch the span a great deal to reach the actual optimum.

2. As span is increases, so does wing bending which can negatively affect stability and flutter characteristics.

3. The cost of the wing itself increases as the structural weight increases.

4. The volume of the wing in which fuel can be stored is reduced.

5. It becomes more difficult to locate the main landing gear at the root of the wing.

6. The Reynolds number of wing sections is reduced, increasing parasite drag and reducing

7. Span might be restricted by the infrastructure (airport gates, hangars) maximum lift capability.

6.1.2 Area

The wing area, like the span, is chosen based on several considerations including:

- Cruise drag
- Stalling speed and field length requirements
- Wing structural weight
- Fuel volume

These considerations often lead to a wing with the smallest area allowed by the constraints. But this is not always true; sometimes the wing area must be increased to obtain a reasonable C_L at the selected cruise conditions.

Selecting cruise conditions is also an integral part of the wing design process. It should not be dictated a priori because the wing design parameters will be strongly affected by the selection, and an appropriate selection cannot be made without knowing some of these parameters. But the wing designer does not have complete freedom to choose these, either. Cruise altitude affects the fuselage structural design and the engine performance as well as the aircraft aerodynamics. The best C_L for the wing is not the best for the aircraft as a whole. An example of this is seen by considering a fixed C_L, fixed Mach design. If we fly higher, the wing area must be increased by the wing drag is nearly constant. The fuselage drag decreases, though; so we can minimize drag by flying very high with very large wings. This is not feasible because of considerations such as engine performance.

Aspect ratio is directly related to the wing area and wing span and is defined as:

$$AR = \frac{b^2}{S_{\text{ref}}}, \tag{6.1}$$

where S_{ref} should be the same as the one used in the definition of C_L and C_D.

6.1.3 Sweep

Sweep is the angle between the $c/4$ line and the spanwise axis. Wing sweep is mainly used for reducing transonic wave drag. There are cases, however, when sweep is used to improve stability (as in the case of flying wings).

Sweep has the following consequences:

- It permits higher cruise Mach number, greater airfoil thickness or higher C_L at a given Mach number without drag divergence.
- It increases the additional loading at the tip,
- It increases the structural weight, because of the increased tip loading, and also because of the increased structural span.
- It stabilizes the wing aeroelastically but is destabilizing to the airplane.
- Too much sweep makes it difficult to accommodate the main gear in the wing.

Much of the effect of sweep varies as the cosine of the sweep angle, making forward and aft-swept wings similar. There are, however, important differences in other characteristics.

6.1.4 Thickness

The distribution of thickness from wing root to tip is selected by considering the following:

- We would like to make t/c as large as possible to reduce wing weight
- Greater t/c tends to increase $C_{L_{\max}}$ up to a point, depending on the high-lift system, but gains above about 12% are small if there at all.
- Greater t/c increases fuel volume and wing stiffness.
- Increasing t/c increase incompressible drag slightly by increasing the velocities and the adversity of the pressure gradients.
- Increasing t/c shifts the transonic drag rise towards lower the Mach numbers, limiting the speed and C_L at which the airplane may fly efficiently.

6.1.5 Taper

Wing taper is the ratio of tip cord to root chord, i.e.,

$$\lambda = \frac{c_{\text{tip}}}{c_{\text{root}}} \tag{6.2}$$

The wing taper ratio (and planform shape in general) is determined from the following considerations:

- The planform shape should not give rise to an additional lift distribution that is so far from elliptical that the required twist for low cruise drag results in large off-design penalties.
- The chord distribution should be such that with the cruise lift distribution, the distribution of lift coefficient is compatible with the section performance. Avoid high C_ls which may lead to buffet, drag rise, or separation.

- The chord distribution should produce a load distribution which is compatible with the high-lift system and desired stalling characteristics.
- Lower taper ratios lead to lower wing weight.
- Lower taper ratios result in increased fuel volume.
- The tip chord should not be too small as Reynolds number effects cause reduced C_l capability.
- Larger root chords more easily accommodate landing gear.

The major design goal is to keep the taper ratio as small as possible (to keep the wing weight down) without excessive C_l variation or unacceptable stalling characteristics. Since the lift distribution elliptical, the chord distribution should be nearly elliptical for a uniform C_l distribution.

6.1.6 Twist

The twist must be chosen so that the cruise drag is low.

Other considerations include:

- Extra washout (negative twist towards the wing tip) helps the stalling characteristics.
- Twist changes the structural weight by modifying the moment distribution over the wing.
- Twist on swept-back wings also produces a positive pitching moment which has a small effect on trimmed drag.

The selection of wing twist is therefore accomplished by examining the trades between cruise drag, drag in second segment climb, and the wing structural weight. The selected washout is then just a bit higher to improve stall.

6.2 Lift Distributions

It is easier to relate the wing geometry to its performance through the intermediary of the lift distribution. Wing design often proceeds by selecting a desirable wing lift distribution and then finding the geometry that achieves this distribution. In this section, we describe the lift and lift coefficient distributions, and relate these to the wing geometry and performance.

6.2.1 Lift and C_l Distributions

The distribution of lift on the wing affects the wing performance in many ways. The lift per unit length $l(y)$ may be plotted from the wing root to the tip as shown below.

In this case the distribution is roughly elliptical. In general, the lift goes to zero at the wing tip. The area under the curve is the total lift. The section lift coefficient is related to the section lift by

$$C_l(y) = \frac{l(y)}{qc(y)}. \tag{6.3}$$

Thus, if we know the lift distribution and the planform shape, we can find the C_l distribution: The lift and lift coefficient distributions are directly related by the chord distribution.

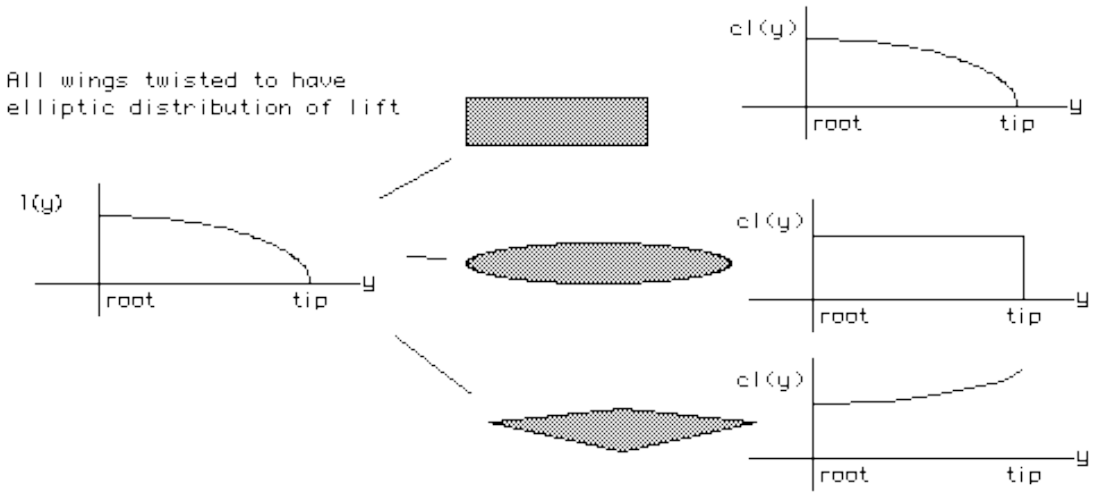

Figure 6.2: Relating lift and lift coefficient distributions: The lift distribution on the left can yield all three lift coefficient distributions on the left, depending on the chord distribution.

6.2.2 Wing Geometry and Lift Distributions

The wing geometry affects the wing lift and C_l distributions in ways that are intuitive for the most part.

Increasing the taper ratio (making the tip chords larger) produces more lift at the tips, just as one might expect, but because the section C_l is the lift divided by the local chord, taper has a very different effect on the C_l distribution.

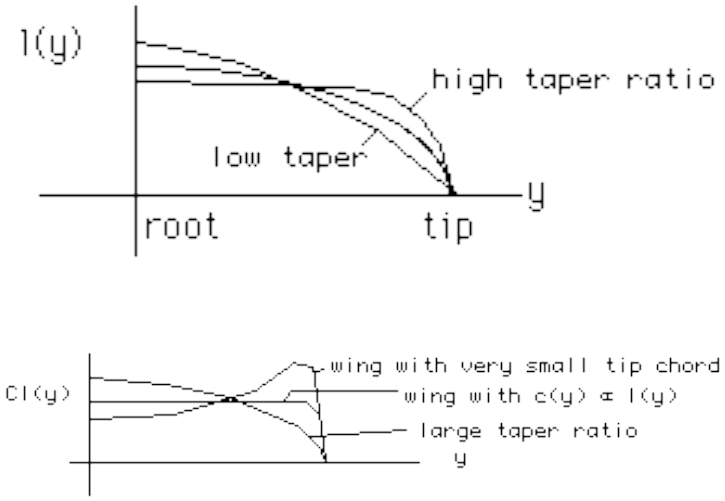

When it comes to wing twist, increasing the tip incidence with respect to the root is called wash-in. Wings often have less incidence at the tip than the root (wash-out) to reduce structural weight and improve stalling characteristics. Since changing the wing twist does not affect the chord distribution, the effect on lift and C_l is similar.

Wing sweep produces a less intuitive change in the lift distribution of a wing. Because the downwash velocity induced by the wing wake depends on the sweep, the lift distribution is affected.

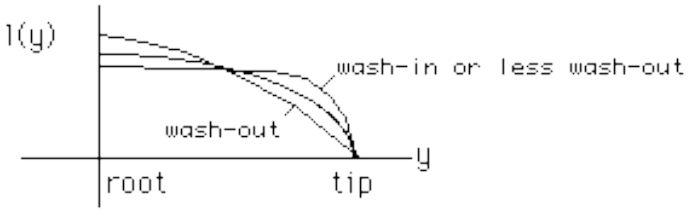

The result is an increase in the lift near the tip of a swept-back wing and a decrease near the root (as compared with an unswept wing). This effect can be quite large and causes problems for swept-back wings. The greater tip lift increases structural loads and can lead to stalling problems.

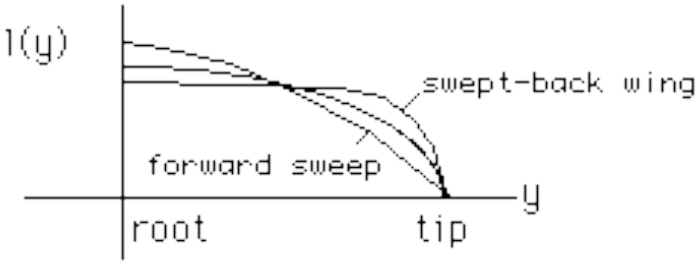

Note that many of these effects are similar and by combining the right twist and taper and sweep, we can achieve desirable distributions of lift and lift coefficient. For example: Although a swept back wing tends to have extra lift at the wing tips, wash-out tends to lower the tip lift. Thus, a swept back wing with washout can have the same lift distribution as an unswept wing without twist.

Lowering the taper ratio can also cancel the influence of sweep on the lift distribution. However, then the C_l distribution is different. Today, we can relate the wing geometry to the lift and C_l distributions with panel methods. Yet, this more intuitive understanding of the impact of wing parameters on the distributions remains an important skill.

6.2.3 Lift Distributions and Performance

Wing design has several goals related to the wing performance and lift distribution. One would like to have a distribution of C_l that is relatively flat so that the airfoil sections in one area are not "working too hard" while others are at low C_l. In such a case, the airfoils with C_l much higher than the average will likely develop shocks sooner or will start stalling prematurely.

The induced drag depends solely on the lift distribution, so one would like to achieve a nearly elliptical distribution of section lift.

On the other hand structural weight is affected by the lift distribution as well, so the ideal shape depends on the relative importance of induced drag and wing weight.

By varying taper, sweep, and twist, these goals can be easily achieved at a given design point. The difficulty appears when the wing must perform well over a range of conditions. One of the more interesting tradeoffs that is often required in the design of a wing is that between drag and structural weight. This may be done in several ways. Some of the optimization problems that have been solved include:

- Minimum induced drag with given span (Prandtl)
- Minimum induced drag with given root bending moment (Jones, Lamar, and others)
- Minimum induced drag with fixed wing weight and constant thickness (Prandtl, Jones)
- Minimum induced drag with given wing weight and specified thickness-to-chord ratio (Ward, McGeer, Kroo)
- Minimum total drag with given wing span and planform – Kuhlman
- Maximum range and other problems based on the Breguet range equation

There are many problems of this sort left to solve and many approaches to the solution of such problems. These include some closed-form analytic results, analytic results together with iteration, and finally numerical optimization.

The best wing design will depend on the construction materials, the arrangement of the high-lift devices, the flight conditions (C_L, Re, M) and the relative importance of drag and weight.

All of this is just to say that it is difficult to design just a wing without designing the entire airplane. If we were just given the job of minimizing cruise drag the wing would have a very high aspect ratio.

If we add a constraint on the wing structural weight based on a trade-off between cost and fuel savings then the problem is somewhat better posed but we would still select a wing with very small taper ratio.

High t/c and high sweep are often suggested by studies that include only weight and drag. The high lift characteristics of the design force the taper ratio and sweep to more usual values and therefore must be a fundamental consideration at the early stages of wing design. Unfortunately the estimation of $C_{L_{\max}}$ is one of the more difficult parts of the preliminary design process.

6.3 Winglets and Other Nonplanar Wings

Increasing the wing span redistributes the spanwise vorticity such that induced drag is reduced. Winglets have a similar effect.

However, when the wing-winglet combination is optimized for minimum drag at fixed span, it achieves about the same drag as a planar wing with a span increased by about 45% of the winglet height.

The same approach may be taken for general nonplanar wake shapes. The figure below summarizes some of these results.

Several points should be made about the preceding results:

- The result that the sidewash on the winglet is zero for minimum induced drag means that the self-induced drag of the winglet just cancels the winglet thrust associated with wing sidewash. Optimally-loaded winglets thus reduce induced drag by lowering the average downwash on the wing, not by providing a thrust component.
- The results shown here deal with the inviscid flow over nonplanar wings. There is a slight difference in optimal loading in the viscous case due to lift-dependent viscous drag.
- Other potentially important factors not considered in this study are: stability and control, structures, and a number of practical issues.

More details on the design of nonplanar wings may be found in various papers (Jansen et al., 2010; Kroo, 2005; Kroo et al., 1998; Verstraeten and Slingerland, 2009; **?**).

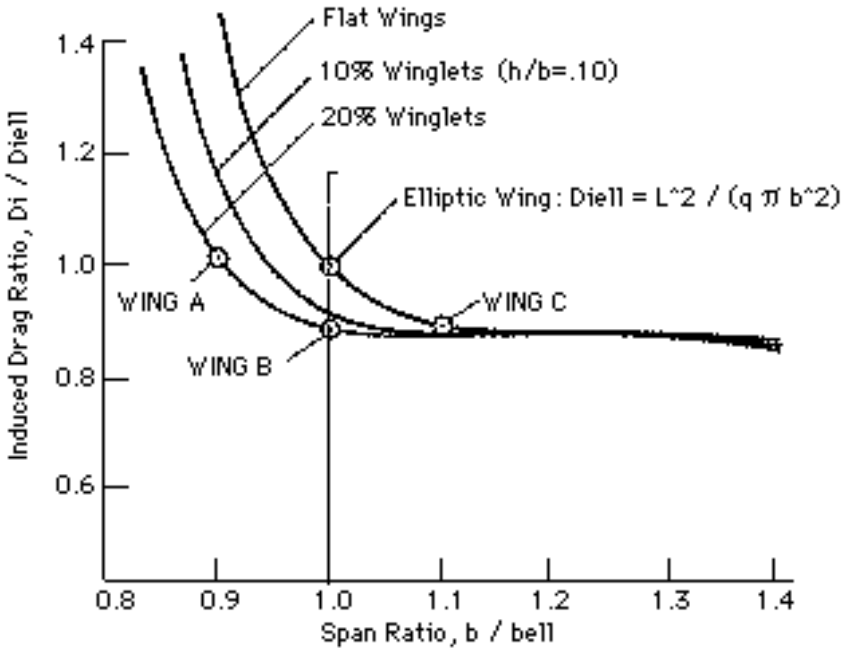

Figure 6.3: Span efficiency of different wings for varying span

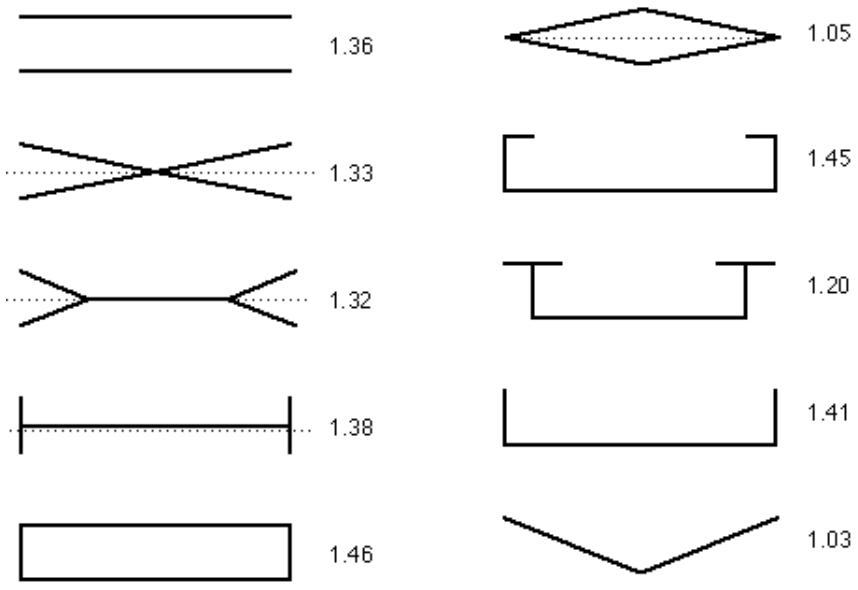

Figure 6.4: Maximum span efficiency for nonplanar wings of various shapes with a height to span ratio of 0.2

6.4 Transonic Wave Drag

We now present an alternative approach to Raymer (2006, Figs. 12.28–12.33). This approach relies on the prediction of wave drag, rather than directly deciding the design parameters. It uses the three-dimensional version of the Korn equation, which can be used to predict the wave drag of swept wings (Malone and Mason, 1995). The Korn equation connects the drag divergence Mach number with airfoil performance, wing sweep and thickness-to-chord ratio by the following relation:

$$M_{DD} = \frac{\kappa}{\cos\Lambda} - \frac{t/c}{\cos^2\Lambda} - \frac{C_L}{10\cos^3\Lambda} \tag{6.4}$$

where M_{DD} is the drag divergent Mach number, C_L is the wing lift coefficient in cruise, Λ is the wing sweep at the quarter chord, t/c is the average wing thickness-to-chord ratio, and κ is an *airfoil technology factor*. This factor varies from $\kappa = 0.87$ for a NACA 6-series airfoil section, to $\kappa = 0.95$ for a supercritical section (Mason, 1990).

The critical Mach number is the minimum Mach number for which there is sonic flow over any portion of the wing, and is determined empirically by

$$M_{\text{crit}} = M_{DD} - \left(\frac{0.1}{80}\right)^{1/3} \tag{6.5}$$

The wave drag coefficient can then be estimated by:

$$C_{D\text{wave}} = 20\,(M - M_{\text{crit}})^4 \tag{6.6}$$

which is valid if $M > M_{\text{crit}}$. If $M < M_{\text{crit}}$, there are no shocks and the wave drag is zero.

6.5 Airfoil Design

6.5.1 Airfoil Geometry

Airfoil geometry can be characterized by the coordinates of the upper and lower surface. It is often summarized by a few parameters such as: maximum thickness, maximum camber, position of maximum thickness, position of max camber, and nose radius. One can generate a reasonable airfoil section given these parameters. This was done by Eastman Jacobs in the early 1930's to create a family of airfoils known as the NACA Sections.

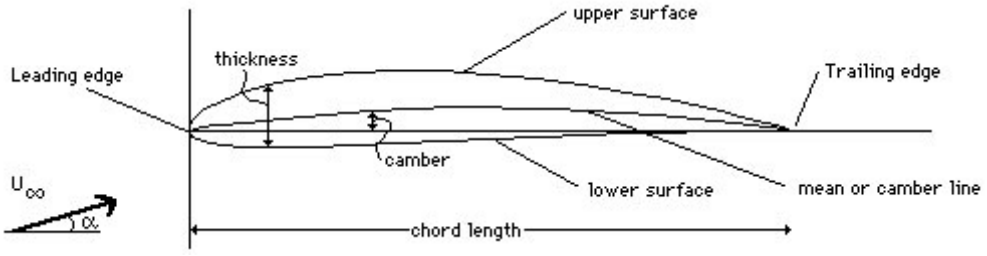

Figure 6.5: Airfoil geometry parameters

The NACA 4 digit and 5 digit airfoils were created by superimposing a simple meanline shape with a thickness distribution that was obtained by fitting a couple of popular airfoils of the time:

$$\pm y = \frac{t}{0.2}\left(.2969x^{1/2} - .126x - .3537x^2 + .2843x^3 - .1015x^4\right) \tag{6.7}$$

Table 6.1: NACA 4-Digit Series

4	4	12
max camber in % c	position of max camber in 1/10 of c	max t/c in %

Table 6.2: NACA 5-Digit Series

2	30	12
approx max camber in % c	position of max camber in 2/100 of c	max t/c in %

The camberline of 4-digit sections was defined as a parabola from the leading edge to the position of maximum camber, then another parabola back to the trailing edge.

After the 4-digit sections came the 5-digit sections such as the famous NACA 23012. These sections had the same thickness distribution, but used a camberline with more curvature near the nose. A cubic was faired into a straight line for the 5-digit sections.

The 6-series of NACA airfoils departed from this simply-defined family. These sections were generated from a more or less prescribed pressure distribution and were meant to achieve some laminar flow.

After the 6-series sections, airfoil design became much more specialized for the particular application. Airfoils with good transonic performance, good maximum lift capability, very thick sections, very low drag sections are now designed for each use. Often a wing design begins with the definition of several airfoil sections and then the entire geometry is modified based on its 3-dimensional characteristics.

6.5.2 Airfoil Pressure Distributions

The aerodynamic performance of airfoil sections can be studied most easily by reference to the distribution of pressure over the airfoil (just like referring to the spanwise lift distribution to study the effect of planform variables on the wing aerodynamic performance). This distribution is usually expressed in terms of the pressure coefficient (C_p), which is the difference between local static pressure and freestream static pressure, nondimensionalized by the freestream dynamic pressure, i.e.,

$$C_p = \frac{p - p_\infty}{\frac{1}{2}\rho U_\infty^2}. \tag{6.8}$$

What does an airfoil pressure distribution look like? We generally plot C_p vs. x/c.

x/c varies from 0 at the leading edge to 1.0 at the trailing edge. C_p is plotted "upside-down" with negative values (suction), higher on the plot. (This is done so that the upper surface of a

Table 6.3: NACA 6-Digit Series

6	3	2	–	2	12
Six-series	location of min C_p in 1/10 c	half width of low drag bucket in 1/10 of C_l		ideal C_l in tenths	max t/c in %

conventional lifting airfoil corresponds to the upper curve.)

The C_p starts from about 1.0 at the stagnation point near the leading edge. It rises rapidly (pressure decreases) on both the upper and lower surfaces, and finally recovers to a small positive value of Cp near the trailing edge.

Various parts of the pressure distribution are depicted in the figure below and are described in the following sections.

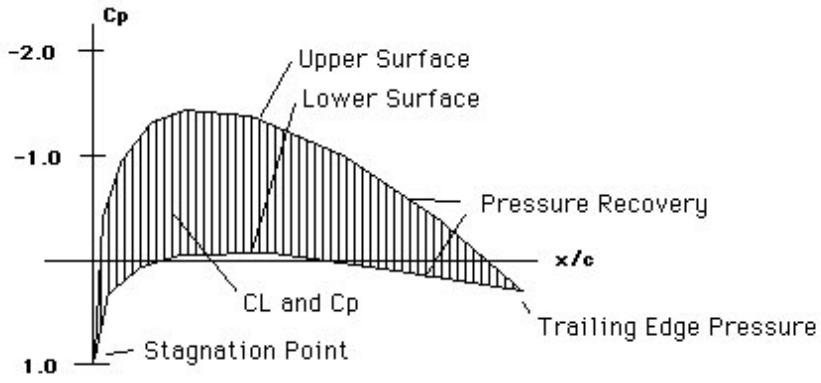

Figure 6.6: Airfoil pressure coefficient

Upper Surface: The upper surface pressure is lower (plotted higher on the usual scale) than the lower surface C_p in this case. But it doesn't have to be.

Lower Surface: The lower surface sometimes carries a positive pressure, but at many design conditions is actually pulling the wing downward. In this case, some suction (negative C_p results in downward force on lower surface) is present near the midchord.

Pressure Recovery: This region of the pressure distribution is called the pressure recovery region. The pressure increases from its minimum value to the value at the trailing edge. This area is also known as the region of adverse pressure gradient. As discussed in other sections, the adverse pressure gradient is associated with boundary layer transition and possibly separation, if the gradient is too severe.

Trailing Edge Pressure: The pressure at the trailing edge is related to the airfoil thickness and shape near the trailing edge. For thick airfoils the pressure here is slightly positive (the velocity is a bit less than the freestream velocity). For infinitely thin sections $C_p = 0$ at the trailing edge. Large positive values of C_p at the trailing edge imply more severe adverse pressure gradients.

C_L and C_p: The section lift coefficient is related to the C_p by:

$$C_l = \int_0^1 (C_{p_l} - C_{p_u}) \, \mathrm{d}\left(\frac{x}{c}\right) \tag{6.9}$$

This represents the area between the curves.

Stagnation Point: The stagnation point occurs near the leading edge. It is the place at which $U = 0$. Note that in incompressible flow $C_p = 1.0$ at this point. In compressible flow it may be somewhat larger.

We can get a more intuitive picture of the pressure distribution by looking at some examples and this is done in some of the following sections in this chapter.

6.5.3 Airfoil Pressures and Performance

The shape of the pressure distribution is directly related to the airfoil performance as indicated by some of the features shown in the Fig. 6.7.

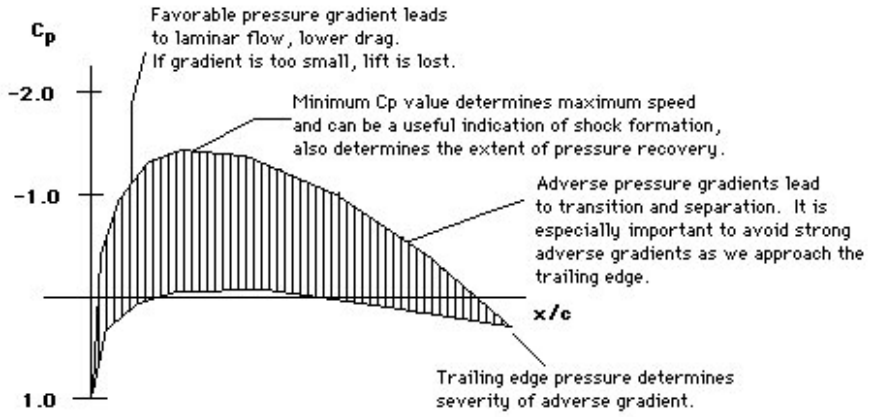

Figure 6.7:

Most of these considerations are related to the airfoil boundary layer characteristics which we will take up later, but even in the inviscid case we can draw some conclusions. We may compute the maximum local Mach numbers and relate those to lift and thickness; we can compute the pitching moment and decide if that is acceptable.

Whether we use the inviscid pressures to form qualitative conclusions about the section, or use them as input to a more detailed boundary layer calculation, we must first investigate the close relation between the airfoil geometry to these pressures.

Relating Airfoil Geometry and Pressures

The relationship between airfoil geometry and airfoil pressure distributions can be predicted numerically solving the relevant field equations. But it can also be understood in an intuitive way.

Let's consider, in more detail the relationship between airfoil geometry and airfoil pressure distributions. The next few examples show some of the effects of changes in camber, leading edge radius, trailing edge angle, and local distortions in the airfoil surface.

6.5.4 Airfoil Design Methods

The process of airfoil design proceeds from a knowledge of the boundary layer properties and the relation between geometry and pressure distribution. The goal of an airfoil design varies. Some airfoils are designed to produce low drag (and may not be required to generate lift at all.) Some sections may need to produce low drag while producing a given amount of lift. In some cases, the drag doesn't really matter — it is maximum lift that is important. The section may be required to achieve this performance with a constraint on thickness, or pitching moment, or off-design

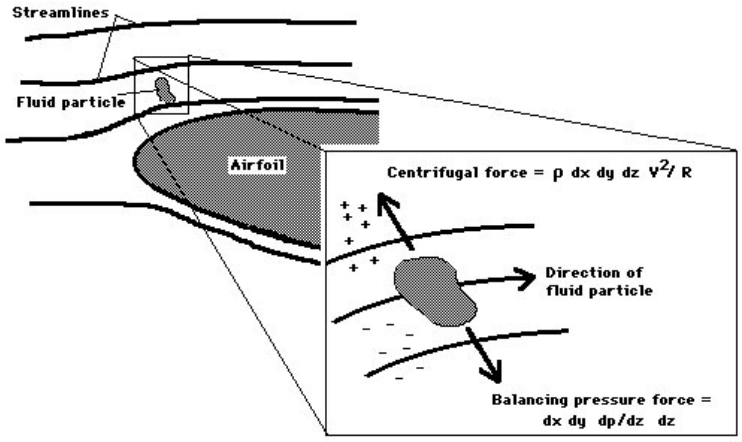

Figure 6.8: Effect of changes in surface curvature

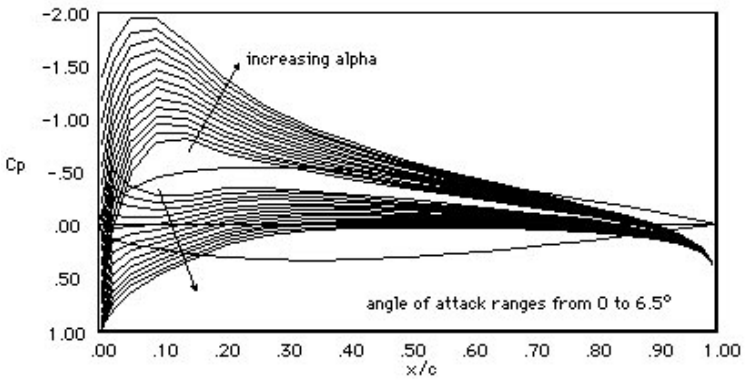

Figure 6.9: Variation of C_p with angle of attack. Note that the "nose peak" becomes more extreme as the angle increases

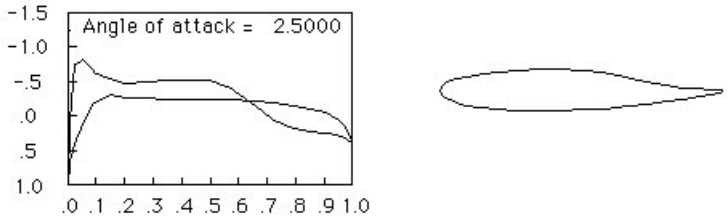

Figure 6.10: A reflexed airfoil section has reduced camber over the aft section producing less lift over this region. and therefore less nose-down pitching moment. In this case the aft section is actually pushing downward and C_{m_0} is positive

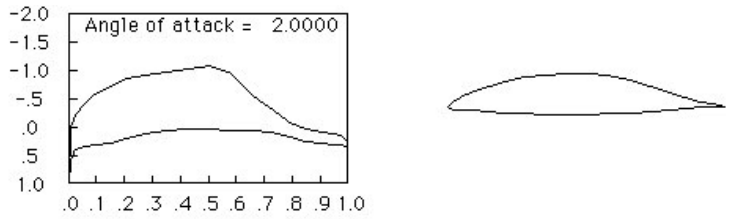

Figure 6.11: A natural laminar flow section has a thickness distribution that leads to a favorable pressure gradient over a portion of the airfoil. In this case, the rather sharp nose leads to favorable gradients over 50% of the section.

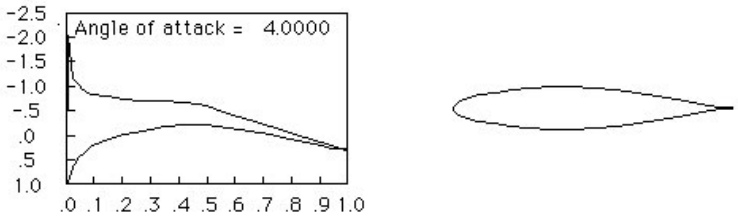

Figure 6.12: Symmetrical section at 4° angle of attack. Note the pressure peak near the nose. A thicker section would have a less prominent peak.

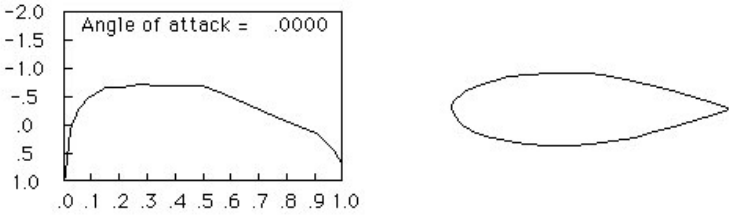

Figure 6.13: Thicker section at 0°. Only one line is shown on the plot because at zero lift, the upper and lower surface pressure coincide.

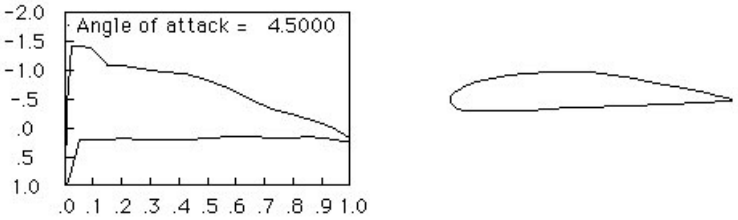

Figure 6.14: A conventional cambered section.

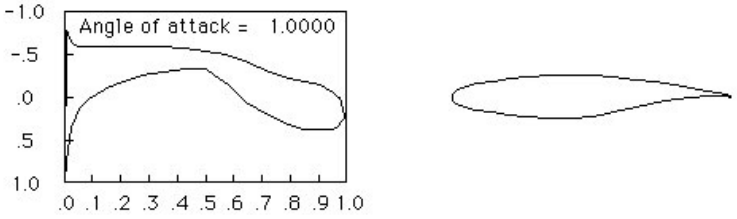

Figure 6.15: Aft-loaded section, the opposite of a reflexed airfoil carries more lift over the aft part of the airfoil. Supercritical airfoil sections look similar to this.

performance, or other unusual constraints. Some of these are discussed further in the section on historical examples.

One approach to airfoil design is to use an airfoil that was already designed by someone who knew what they were doing. This "design by authority" works well when the goals of a particular design problem happen to coincide with the goals of the original airfoil design. This is rarely the case, although sometimes existing airfoils are good enough. In these cases, airfoils may be chosen from catalogs such as Abbott and Von Doenhoff (1959), Althaus and Wortmann (1981), Selig et al. (1989).

The advantage to this approach is that there is test data available. No surprises, such as a unexpected early stall, are likely. On the other hand, available tools are now sufficiently refined that one can be reasonably sure that the predicted performance can be achieved. The use of "designer airfoils" specifically tailored to the needs of a given project is now very common. This section of the notes deals with the process of custom airfoil design.

Methods for airfoil design can be classified into two categories: direct and inverse design.

Direct Methods for Airfoil Design

The direct airfoil design methods involve the specification of a section geometry and the calculation of pressures and performance. One evaluates the given shape and then modifies the shape to improve the performance.

The two main subproblems in this type of method are:

1. The identification of the measure of performance

2. The approach to changing the shape so that the performance is improved

The simplest form of direct airfoil design involves starting with an assumed airfoil shape (such as a NACA airfoil), determining the characteristic of this section that is most problematic, and fixing this problem. This process of fixing the most obvious problems with a given airfoil is repeated until there is no major problem with the section. The design of such airfoils, does not require a specific definition of a scalar objective function, but it does require some expertise to identify the potential problems and often considerable expertise to fix them.

Sometimes the objective of airfoil design can be stated more positively than, "fix the worst things". We might try to reduce the drag at high speeds while trying to keep the maximum C_L greater than a certain value. This could involve slowly increasing the amount of laminar flow at low C_ls and checking to see the effect on the maximum lift. The objective may be defined numerically. We could actually minimize C_d with a constraint on $C_{l_{\max}}$. We could maximize L/D or $C_l^{3/2}/C_d$ or $C_{l_{\max}}/C_{d_{@\text{ design } C_l}}$. The selection of the figure of merit for airfoil sections is quite important and generally cannot be done without considering the rest of the airplane. For example, if we wish to build an airplane with maximum L/D we do not build a section with maximum L/D because the section C_l for best C_l/C_d is different from the airplane C_L for best C_L/C_D.

Inverse Design

Another type of objective function is the target pressure distribution. It is sometimes possible to specify a desired C_p distribution and use the least squares difference between the actual and target C_ps as the objective. This is the basic idea behind a variety of methods for inverse design. As an example, thin airfoil theory can be used to solve for the shape of the camberline that produces a specified pressure difference on an airfoil in potential flow.

The second part of the design problem starts when one has somehow defined an objective for the airfoil design. This stage of the design involves changing the airfoil shape to improve the performance. This may be done in several ways:

1. By hand, using knowledge of the effects of geometry changes on C_p and C_p changes on performance.

2. By numerical optimization, using shape functions to represent the airfoil geometry and letting the computer decide on the sequence of modifications needed to improve the design.

Bibliography

Ira Herbert Abbott and Albert Edward Von Doenhoff. *Theory of wing sections, including a summary of airfoil data*. Dover Publications, New York, 1959.

Dieter Althaus and Franz Xaver Wortmann. *Stuttgarter Profilkatalog*. F. Vieweg, Braunschweig, Germany, 1981.

John D. Anderson Jr. *Aircraft Performance and Design*. McGraw–Hill, 1999.

Peter Jansen, Ruben. E. Perez, and Joaquim R. R. A. Martins. Aerostructural optimization of nonplanar lifting surfaces. *Journal of Aircraft*, 47(5):1491–1503, September 2010. doi:10.2514/1.44727.

Ilan Kroo. Nonplanar wing concepts for increased aircraft efficiency. In *VKI lecture series on Innovative Configurations and Advanced Concepts for Future Civil Aircraftecture series on Innovative Configurations and Advanced Concepts for Future Civil Aircraft*, 2005.

Ilan Kroo, John McMasters, and Stephen C. Smith. Highly nonplanar lifting systems. In *Transportation Beyond 2000: Technologies Needed for Engineering Design*, pages 331–370, September 1998.

B. Malone and W.H. Mason. Multidisciplinary optimization in aircraft design using analytic technology models. *Journal of Aircraft*, 32(2):431–438, mar-apr 1995. doi:10.2514/3.46734.

W. H. Mason. Analytic models for technology integration in aircraft design. In *AIAA/AHS/ASEE Aircraft Design, Systems and Operations Conference*, Dayton, OH, September 1990. doi:10.2514/6.1990-3262. AIAA 1990-3262.

Daniel P. Raymer. *Aircraft Design: A Conceptual Approach*. AIAA, 4th edition, 2006.

Michael S Selig, John Francis Donovan, and David B Fraser. *Airfoils at low speeds*, volume 8. H.A. Stokely, Virginia Beach, Va., USA (1504 Horseshoe Cir., Virginia Beach 23451), 1989.

Joram G. Verstraeten and Ronald Slingerland. Drag characteristics for optimally span-loaded planar, wingletted, and C wings. *Journal of Aircraft*, 46(3):962–971, 2009.